MEMS Strain Sensors with High Linearity and Sensitivity with an Enhanced Strain Transfer Mechanism for Wind Turbine Blades

M. Moradi and S. Sivoththaman

Department of Electrical and Computer Engineering, University of Waterloo.
200 University Avenue West, Waterloo, Ontario N2L 3G1, Canada. m3moradi@uwaterloo.ca

ABSTRACT

A new physical sensor design for strain measurement of wind turbine blades is presented. While the proposed structure is highly sensitive, it is based on simple operating principle of displacement amplification. The proposed microdevice converts even small amount of applied strains to measurable changes in capacitance. The device performance is validated both by analytical solution and also by finite element methods (FEM). Moreover, to address the influence of the adhesive layer used for bonding the sensor to wind turbine blades on strain transmission, the ratio of strain transmission is investigated through FEM simulation and finally a technique is proposed that increases this ratio by up to 30%.

Keywords: microelectromechanical, strain sensor, comb-drive, finite element method, strain transmission.

1 INTRODUCTION

Blade strain is one of the most important quantities to judge the health of wind turbine structure. High or long lasting strain may lead to crack formation, yielding, or fatigue in the structure material. Therefore, high performance strain measurement system, consisting of sensors and interface electronics, is highly desirable. Research on wind turbine load measurement has been carried out for many years and it has been revealed that the conventional strain gauge technique exhibits significant errors and uncertainties when applied to composite materials of wind turbine blades. Sensing and control mechanisms deploying devices based on microelectromechanical systems (MEMS) lead to smart condition monitoring systems that ensure safe operation of wind turbines through intelligent sensing components. At the same time lower costs in the development of MEMS sensors and their compatibility for integration with CMOS technology for data processing and controls are the key factors to achieve the reliability goals.

Conventional strain sensors made of piezoresistive elements or metal foils are inadequate for high performance and low cost applications due to their large temperature dependence, low sensitivity, and incompatibility to standard CMOS integration. Capacitive MEMS strain sensors, however, can be monolithically integrated with low power CMOS electronics [1] and also are desirable because of low temperature dependence and high sensitivity.

In this work, a strain sensing microdevice with high sensitivity and adequate linearity is presented. The structure is composed of differential capacitive strain sensing and mechanical amplification mechanism. The strain measurement resolution of this sensor is 40 με/fF up to a maximum strain of ±3000 με. This performance represents improvement compared to existing MEMS strain sensors [2] and at the same time has a simpler structure design. The large range of strain measurement is favorable in wind turbine blade strain sensing, however, this causes some loss in sensitivity.

2 DISPLACEMENT AMPLIFICATION

The principle of operation the displacement amplification microdevice is as follows: application of an input force, which is the strain transferred to the sensor substrate from the wind turbine blade, will generate deformation of a flexure-based mechanism, the input displacement created by this force will be amplified in another direction where comb-drive-like structure capacitors are placed. The proposed structure converts small amount of applied strains to measurable changes in capacitance. Figure 1 depicts the concept of displacement amplification.

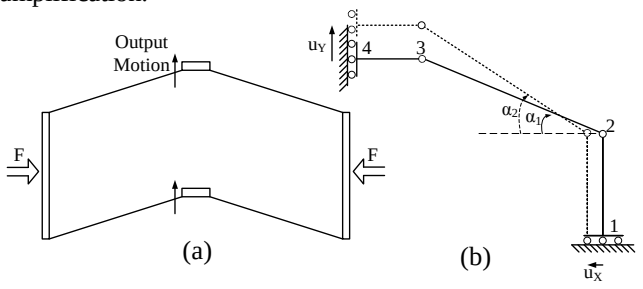

Figure 1: a) Displacement amplification microdevice with four straight flexures. b) Amplification mechanism with the simplifying assumption that the flexures are always straight.

The mechanical gain of the above configuration is a function of the main flexure length, its mechanical properties, and the original inclination angle. The exact

analysis based on input and output stiffness and assuming that the main links are straight beams, is presented in the following section.

3 CAPACITIVE STRAIN SENSOR

Figure 2 presents the architecture of the proposed microdevice composed of four straight beams to convert the strain-produced horizontal displacement to vertical movement and also perform mechanical amplification to enhance the device sensitivity. Beams are connected to interdigitated fingers creating capacitors with fixed top and bottom electrodes. Small horizontal displacement caused by the external strain Δx is converted to vertical direction and amplified by the mechanical gain $\Delta y=\alpha\Delta x$. Moving the fingers will change the capacitance of differential sensing capacitors. The beams are designed with 200 µm length, 3 µm width, and original inclination angle of 10°. Finger electrodes have 120 µm length, 3 µm width and 5 µm height. The air gap distance between the finger electrodes and fixed electrodes are initially 10 µm.

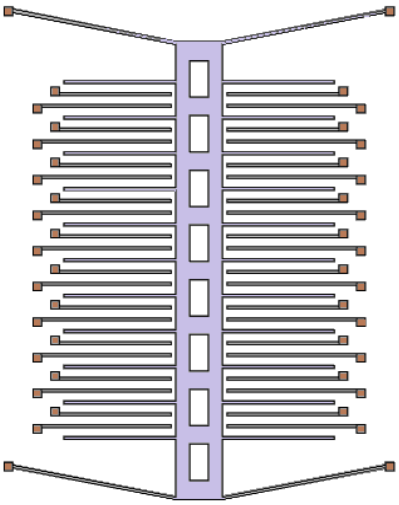

Figure 2: Differential capacitive strain sensor with four mechanical amplifying beams.

To perform the analytical modeling of the structure first we need to calculate the mechanical gain and the vertical movement caused by the beams for a given applied strain. The accurate approach followed here is based on input and output stiffness of one straight beam. So, two reference frames are used, a global frame XY and a local frame with axis aligned with the straight beams. The actuating force caused by the host structure under strain is decomposed locally and consequently we can write the following matrix equation, and therefore obtain the input stiffness [3].

$$\begin{bmatrix} F_{1x} \\ F_{1y} \\ M_1 \end{bmatrix} = \begin{bmatrix} K_{Fx-ux} & 0 & 0 \\ 0 & K_{Fy-uy} & K_{Fy-\theta z} \\ 0 & K_{Fy-\theta z} & K_{Mz-\theta z} \end{bmatrix} \begin{bmatrix} u_{1x} \\ u_{1y} \\ \theta_{1z} \end{bmatrix} \quad (1)$$

$$K = \begin{bmatrix} \frac{EA}{l} & 0 & 0 \\ 0 & \frac{12EI_z}{l^3} & \frac{-6EI_z}{l^2} \\ 0 & \frac{-6EI_z}{l^2} & \frac{4EI_z}{l} \end{bmatrix} \quad (2)$$

$$K_{in} = \frac{F_{in}}{u_{1X}} = \frac{1}{\frac{\cos^2\alpha}{K_{Fx-ux}} + \frac{\sin^2\alpha}{K_{Fy-uy}}} \quad (3)$$

where E, A, l, and I_Z are Young's modulus, cross section, length, and moment of inertia of the beam, respectively. A similar approach can be used for finding the output stiffness and finally the mechanical gain:

$$K_{in} = \frac{F_{out}}{u_{4Y}} = \frac{1}{\frac{\cos^2\alpha}{K_{Fy-uy}} - \frac{\sin^2\alpha}{K_{Fx-ux}}} \quad (4)$$

$$\alpha = \frac{u_{4Y}}{u_{1X}} = \frac{\sin 2\alpha \left(\frac{1}{K_{Fy-uy}} - \frac{1}{K_{Fx-ux}}\right)}{\frac{\sin^2\alpha}{K_{Fy-uy}} + \frac{\cos^2\alpha}{K_{Fx-ux}}} \quad (5)$$

The full microdevice is comprised of four flexures where the left flexure can be considered as the right flexure mirrored about the vertical line, so the stiffness of the left flexure is equal to that of the right one from the mirror operation. Consequently, the overall stiffness of the structure, in a spring-based model, can be thought of as the effective stiffness of the four parallel springs. When the full mechanism is considered, the input displacement is applied from both sides but the output is collected only at the direction perpendicular to the input direction. As a consequence, the amplification of the total microdevice can be calculated as:

$$\alpha_{total} = \frac{u_{in}}{u_{out}} = \frac{u_{4Y}}{2u_{1X}} = a/2 \quad (6)$$

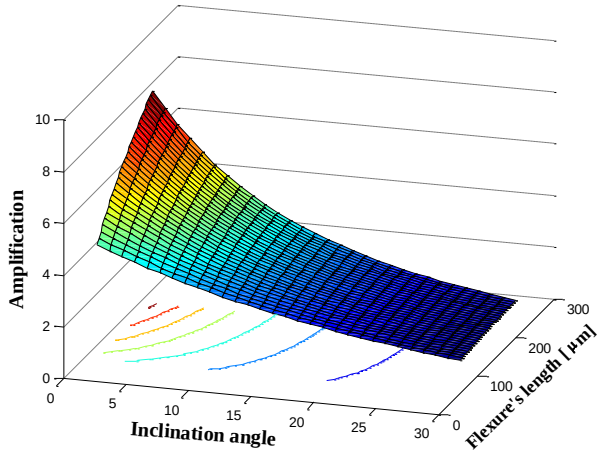

Figure 3: Displacement amplification as a function of the beam's length and inclination angle.

Figure 3 is a plot of amplification in terms of the length of the main flexure and its original inclination angle. As expected, the amplification increases with increasing *l* and with decreasing inclination angle. For an angle of 10° and *l* of 200 µm, displacement amplification is calculated as 2.56.

Finite element method simulation analysis is also carried out using COMSOL Multiphysics®. An external strain of 1000 µε is applied to the substrate and the simulation outcome is depicted in Figure 4 illustrating the vertical movement with respect to the initial position. Almost 25 fF change in total capacitance is observed due to the vertical movement caused by the strain. The displacement amplification is also 2.41 which is close enough to the value obtained by analytical calculations.

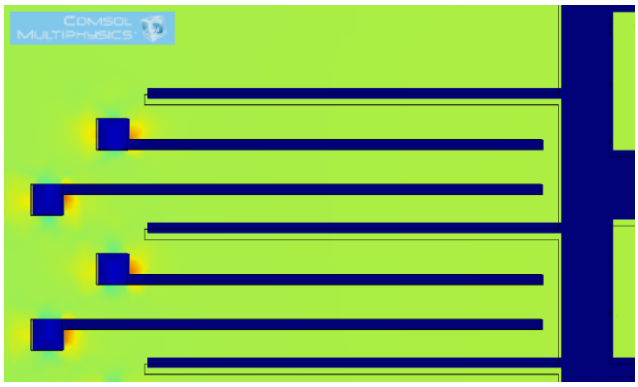

Figure 4: Finite element method simulation of the capacitive sensor and vertical movement of finger electrodes from their original position due to the horizontal strain (red color around anchors is showing higher stress values around this area).

4 STRAIN TRANSMISSION ENHANCEMENT

Once the sensor is fabricated with the desired specifications, in order to transfer the strain from the host structure to the sensor, a bonding layer such as epoxy must be used in between. Most of the researches are based on the assumption that sensors are perfectly bonded to the host structure (i.e. wind turbine blade) and the strain is transferred completely to the sensor. However, since the mechanical interaction between the host structure and the sensor occurs through a layer of adhesive material, the influence of the adhesive layer on strain transmission warrants a more detailed investigation [4].

This section mainly concerns the understanding and study of how loads are transferred from the host structure (i.e. wind turbine blade) to the sensor silicon substrate through an adhesive layer. Finite element method (FEM) simulation using COMSOL Multiphysics® is carried out for Young's moduli of 150 GPa, 170 GPa, and 3.3 GPa, respectfully for composite host structure, silicon substrate, and the adhesive layer. The thickness of the substrate and adhesive layer are 400µm and 100 µm respectively. Finally, it is assumed that external force is applying strain equal to 1000 µε. Figure 5 displays the created three-dimensional finite element model and Figure 6 shows simulation results for strain distributions, with the shear stress in the adhesive layer shown in inset.

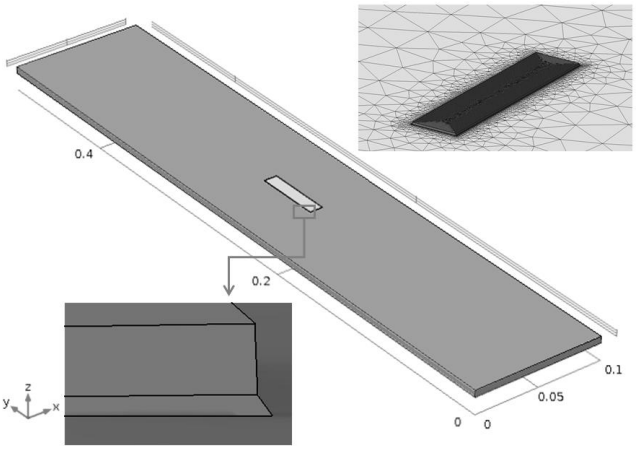

Figure 5: Finite element model of the investigated adhesive bonded structure. Bottom left inset is showing that how the strain from the host structure surface causes deformation of adhesive layer and consequently sensor's silicon substrate.

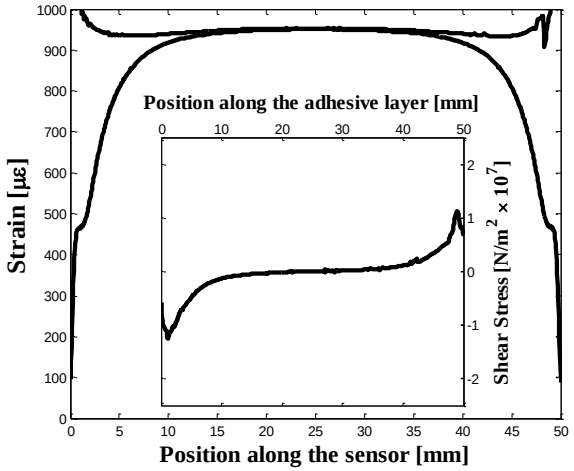

Figure 6: Simulation results for strain distributions and also the existing shear stress in the adhesive layer.

The variation of the sensor strain transfer ratio with adhesive layer thickness for different values of sensor length is shown in Figure 7. It can be observed that higher transfer ratio is obtained at thinner adhesive layers. This figure also clearly demonstrates that variation of adhesive thickness can substantially change the strain transfer ratio at shorter sensor substrates. Figure 7 inset describes the variation of the stain transfer ratio for different Young's moduli and thicknesses of the adhesive layer. From Figure 7, we can conclude that thinner and stiffer adhesive and longer sensor substrates are desirable for achieving higher strain transfer ratio.

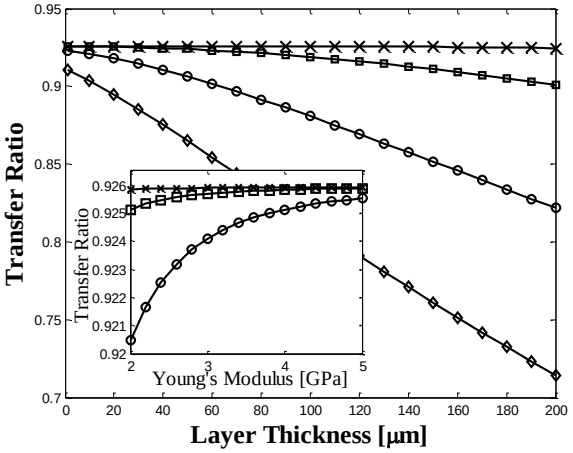

Figure 7: Simulation results describing the influence of adhesive layer thickness on sensor gauge factor at different values of sensor length (*l*=50, 30, 20, 15mm). Inset: Simulation results describing the effect of mechanical properties (Young's Modulus) of the bonding adhesive layer on sensor gauge factor at different values of thicknesses (*t*=50,100,200μm).

Figure 8 depicts the simulation results on the effect of sensor substrate thickness and its Young's modulus on the sensor strain transfer ratio at different sensor lengths. As predicted, the strain transfer ratio decreases when the substrate gets thicker or made by higher modulus materials. Moreover, it was also observed that the strain transfer ratio is more sensitive to the adhesive layer properties when the sensor is bonded on a stiffer substrate.

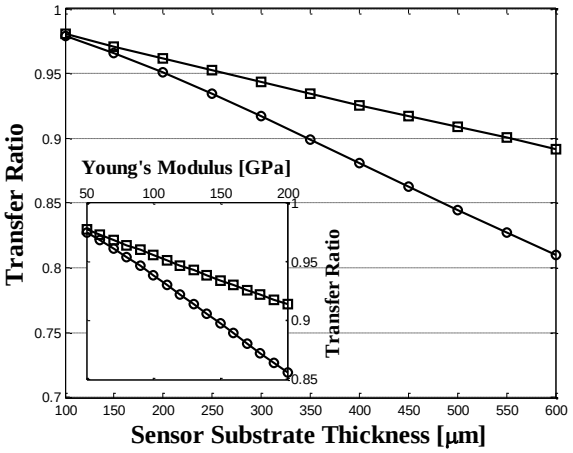

Figure 8: Simulation results describing the effect of sensor substrate thickness. Inset: Effect of substrate Young's Modulus on sensor strain transfer ratio at different values of sensor length.

Finite element method simulation results can be employed to introduce a geometric feature, instead of a flat substrate to enhance the strain transmission ratio. Figure 9 presents the proposed structure with some etched surface trenches on the silicon chip around the sensing MEMS element (e.g. a comb-drive structure). The result of the FEA simulations of these proposed models are also depicted on the figures and compared with the flat chip reference model. Strain transfer enhancement up to 30% is obtained using this technique.

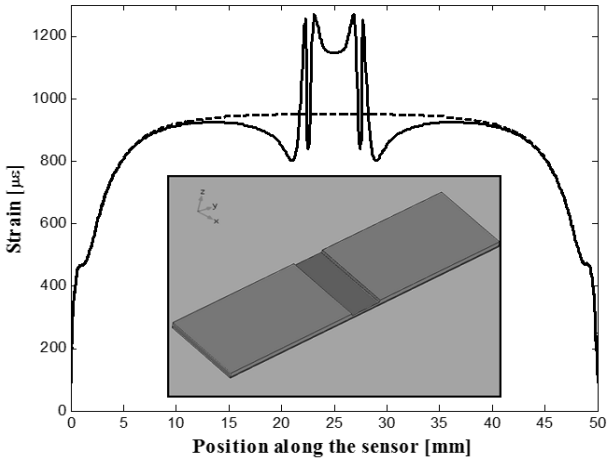

Figure 9: Etched surface trench on the silicon chip is made where the sensing MEMS element is going to be placed. This technique enhances the transferred strain up to 30%.

5 CONCLUSION

A MEMS differential capacitive strain sensor enhanced with displacement amplifying bent-beam is designed. Based on FEM simulation results the design is capable of measuring a strain resolution of 40 με/fF and up to a maximum strain of ±3000 με. It is also found that thinner and stiffer adhesive layers as well as longer, thinner and flexible sensor substrates are desirable for achieving higher and stable sensor gauge factors. The outcome can be also used for calibration of the sensor, instead of doing it experimentally. Finally, a strain transmission enhancement technique is proposed through introduction of a geometrical feature etched on the sensor substrate. This feature magnifies the strain in its proximity where the sensing element can be placed.

REFERENCES

[1] H. Qu, D. Fang, and H. Xie, *IEEE Sensors J.*, vol. 8, no. 9, pp. 1511–8, 2008.

[2] M. Suster, J. Guo, N. Chaimanonart, W.H. Ko, and D.J. Young, *IEEE J. Microelectromech. Syst.*, vol. 15, no. 5, pp. 1069–1077, 2006.

[3] K. B. Lee, "Principles of Microelectromechanical Systems," IEEE Press, 2011.

[4] J. Sirohi and I. Chopra, *Journal of Intelligent Material systems and structures*, vol. 11, no. 4, pp. 246-257, 2000.